Inorganic Chemistry
Article

Inorg. Chem. **2009**, *48*, 11215–11225 **11215**
DOI: 10.1021/ic901530p

Hydrogen-Bond Directed Cyanide-Bridged Molecular Magnets Derived from Polycyanidemetalates and Schiff Base Manganese(III) Compounds: Synthesis, Structures, and Magnetic Properties

Daopeng Zhang,[†,‡] Hailong Wang,[†,‡] Yuting Chen,[‡] Zhong-Hai Ni,[*,‡] Laijin Tian,[‡] and Jianzhuang Jiang[*,†,‡]

[†]*Department of Chemistry, University of Science and Technology Beijing, Beijing 100083, China, and*
[‡]*Department of Chemistry, Shandong University, Jinan 250100, China*

Received August 1, 2009

A series of six new cyanide-bridged heterometallic complexes including two tetranuclear T-like $Fe^{III}Mn^{III}_3$ compounds, $\{[Mn(L^1)(H_2O)]_3[Fe(CN)_5(1\text{-}CH_3im)]\}ClO_4\cdot 1.5H_2O$ (**1**) and $\{[Mn(L^2)(H_2O)]_3[Fe(CN)_5(1\text{-}CH_3im)]\}ClO_4\cdot 3H_2O$ (**2**); two heptanuclear cage-shaped $M^{III}Mn^{III}_6$ (M = Fe, Cr) compounds, $\{[Mn(L^2)(H_2O)]_6[Fe(CN)_6]\}[Fe(CN)_6]\cdot 6CH_3OH$ (**3**) and $\{[Mn(L^2)(H_2O)]_6[Cr(CN)_6]\}[Cr(CN)_6]\cdot 6CH_3OH$ (**4**); and two two-dimensional $M-Mn^{III}$ networks, $\{[H_3O][Mn(L^1)]_2[Fe(CN)_6]\}\cdot 2DMF$ (**5**) and $\{K[Mn(L^1)]_2[Cr(CN)_6]\}\cdot 1.5CH_3CN\cdot CH_3OH$ (**6**) (L^1 = N,N-ethylene-bis(3-methoxysalicylideneiminate, L^2 = N,N-ethylene-bis(3-ethoxysalicylideneiminate) have been successfully assembled from three polycyanidemetalates containing five or six cyanide groups and two manganese(III) building blocks containing bicompartmental Schiff base ligands. The cyanide-bridged polynuclear complexes are self-complementary through a coordinated aqua ligand from one complex and the free O_4 compartment from the neighboring complex, giving supramolecular one-dimensional ladders and three-dimensional networks for **1** and **2** and for **3** and **4**, respectively. Investigation over magnetic susceptibilities of the six complexes reveals the overall ferromagnetic interactions for complexes **1**, **2**, **3**, and **5** and antiferromagnetic interaction for **4** and **6**. Compounds **1**−**4** show some characteristics of metamagnet behavior at low temperatures due to the relatively strong intermolecular hydrogen-bonding interaction. The two complexes with two-dimensional structure exhibit three-dimensional antiferromagnetic ordering with typical metamagnetic behavior below 8.4 K for **5** and 11.5 K for **6**, respectively. The present result appears to add new members to the very few examples of polynuclear clusters exhibiting 3D magnetic ordering relying on intermolecular interactions, to the best of our knowledge, which will be helpful for providing valuable information for the understanding and application of intermolecular hydrogen-bonding interactions in the molecular magnetic materials.

Introduction

In the past three decades, molecular magnetic complexes continue to attract great research interest not only for the purpose of fully elucidating the nature of magnetic coupling, magneto-structural correlation, and some exotic magnetic phenomena but also due to their potential applications in high-tech fields.[1,2] Thus far, significant progress has been made in this direction, as exemplified by the report of a large number of related complexes with novel molecular structure and interesting properties. However, directional design and controlling the synthesis of magnetic complexes with exactly predictable molecular structures and properties are still great challenges since different kinds of interactions and many subtle factors play an integrated and elusive role in determining the molecular structure and tuning magnetic properties. In addition, a clear understanding, skillful utilization, and valuable exploration of intermolecular interactions for assembling molecular magnets remain challenging and interesting tasks.

As one of the most important magnetic systems, cyanide-bridged complexes have received much attention since their molecular topological structures and magnetic coupling nature between neighboring metal ions through the cyanide bridge can be relatively readily controlled and predicted. Several effective strategies have been developed for

*To whom correspondence should be addressed. E-mail: jzjiang@sdu.edu.cn (J.J.).

(1) Kahn, O. *Molecular Magnetism*; VCH: Weinheim, Germany, 1993.

(2) (a) Coronado, E.; Galán-Mascarós, J. R.; Gómez-García, C. J.; Laukhin, V. *Nature* **2000**, *408*, 447. (b) Sato, O.; Kawakami, T.; Kimura, M.; Hishiya, S.; Kubo, S.; Einaga, Y. *J. Am. Chem. Soc.* **2004**, *126*, 13176. (c) Berlinguette, C. P.; Dragulescu-Andrasi, A.; Sieber, A.; Galan-Mascaros, J. R.; Gudel, H.-U.; Achim, C.; Dunbar, K. R. *J. Am. Chem. Soc.* **2004**, *126*, 6222. (d) Shatruk, M.; Dragulescu-Andrasi, A.; Chambers, K. E.; Stoian, S. A.; Bominaar, E. L.; Achim, C.; Dunbar, K. R. *J. Am. Chem. Soc.* **2007**, *129*, 6104.

(3) (a) Ferlay, S.; Mallah, T. R.; Ouahès, P.; Veillet, M. V. *Nature* **1995**, *378*, 701. (b) Entley, W. R.; Girolami, G. S. *Science* **1995**, *268*, 397.

(4) (a) Holmes, S. M.; Girolami, G. S. *J. Am. Chem. Soc.* **1999**, *121*, 5593. (b) Li, D. F.; Clérac, R.; Parkin, S.; Wang, G. B.; Yee, G. T.; Holmes, S. M. *Inorg. Chem.* **2006**, *45*, 5251. (c) Li, D.; Parkin, S.; Wang, G.; Yee, G. T.; Clérac, R.; Wernsdorfer, W.; Holmes, S. M. *J. Am. Chem. Soc.* **2006**, *128*, 4214.

Published on Web 10/26/2009

assembling cyanide-bridged magnetic complexes in the past two decades.[3−25] In this process, manganese(III)−salen complexes containing N_2O_2 equatorial salen-type ligands play an important role due to their facile preparation and large spin state ($S = 2$) as well as the usually negative magnetic anisotropy of the central Mn(III) ions. Generally, the steric effect of salen Schiff base ligands can be tuned through peripheral substitution. In comparison with the widely employed salen Schiff base derivatives with the substituents of Cl, Br, Me, or MeO at the fifth position of the salen ligand,[26] the cyanide-bridged manganese(III) complexes with the substituents at other positions of the salen ligand are relative rare.[27,22a,22b,28,29] Very recently, a series of novel bicompartmental Schiff base ligands such as H_2-3-MeO salen were employed in the assembly of phenoxo-bridged heterometallic 3d−3d and 3d−4f complexes through a step-by-step strategy by means of the different selectivities of their two N_2O_2 and O_4 compartments for different metal ions.[30,31] In addition, the O_4 compartment of one ligand could form hydrogen bonds with the water molecule which is coordinated with the metal ion complexed by the N_2O_2 compartment of another ligand, forming novel supramolecular topological structures.[24d,28,32] However, to the best of our knowledge, construction of magnetic materials with 3D magnetic ordering from bicompartmental Schiff base ligands depending on the combination of hydrogen-bond interactions and the directionality of cyanide coordination bonds has not yet been reported thus far.

In the present paper, we describe the design, synthesis, crystal structures, and magnetic properties of a series of six new cyanide-bridged heterometallic complexes, namely, $\{[Mn(L^1)(H_2O)]_3[Fe(CN)_5(1\text{-}CH_3im)]\}ClO_4\cdot 1.5H_2O$ (**1**), $\{[Mn(L^2)(H_2O)]_3[Fe(CN)_5(1\text{-}CH_3im)]\}ClO_4\cdot 3H_2O$ (**2**), $\{[Mn(L^2)(H_2O)]_6[Fe(CN)_6]\}[Fe(CN)_6]\cdot 6CH_3OH$ (**3**), $\{[Mn(L^2)(H_2O)]_6[Cr(CN)_6]\}[Cr(CN)_6]\cdot 6CH_3OH$ (**4**), $\{[H_3O][Mn(L^1)]_2[Fe(CN)_6]\}\cdot 2DMF$ (**5**), and $\{K[Mn(L^1)]_2[Cr(CN)_6]\}\cdot 1.5CH_3CN\cdot CH_3OH$ (**6**), assembled from two bicompartmental

(5) Hatlevik, O.; Buschmann, W. E.; Manson, J. L.; Miller, J. S. *Adv. Mater*. **1999**, *11*, 914.
(6) (a) Kou, H. Z.; Gao, S.; Zhang, J.; Wen, G. H.; Su, G.; Zheng, R. K.; Zhang, X. X. *J. Am. Chem. Soc*. **2001**, *123*, 11809. (b) Kou, H. Z.; Zhou, B. C.; Gao, S.; Wang, R. J. *Angew. Chem., Int. Ed*. **2003**, *42*, 3288. (c) Kou, H. Z.; Zhou, B. C.; Wang, R. J. *Inorg. Chem*. **2003**, *42*, 7658. (d) Ni, Z. H.; Kou, H. Z.; Zhang, L. F.; Ge, C.; Cui, A. L.; Wang, R. J.; Li, Y.; Sato, O. *Angew. Chem., Int. Ed*. **2005**, *44*, 7742.
(7) (a) Ohba, M.; Kawa, H. O. *Coord. Chem. Rev*. **2000**, *198*, 313. (b) Ghalsasi, P. S.; Kikuchi, K.; Ohba, M.; Okawa, H.; Yakhmi, J. V. *Angew. Chem., Int. Ed*. **2001**, *40*, 4242.
(8) (a) Kurmoo, M.; Kumagai, H. M.; Hughes, S.; J. Kepert, C. *Inorg. Chem*. **2003**, *42*, 6709. (b) Lu, Z.; Wang, X.; Liu, Z.; Liao, B.; Gao, S.; Xiong, R.; Ma, H.; Zhang, D.; Zhu, D. *Inorg. Chem*. **2006**, *45*, 999.
(9) (a) Kashiwagi, T.; Ohkoshi, S. I.; Seino, H.; Mizobe, Y.; Hashimoto, K. *J. Am. Chem. Soc*. **2004**, *126*, 5024. (b) Vos, T. E.; Miller, J. S. *Angew. Chem., Int. Ed*. **2005**, *44*, 241. (c) Glaser, T.; Heidemeier, M.; Weyhermüller, T.; Hoffmann, R. D.; Rupp, H.; Müller, P. *Angew. Chem., Int. Ed*. **2006**, *45*, 2416.
(10) (a) Niel, V.; Thompson, A. L.; Muñoz, M. C.; Galet, A.; Goeta, A. E.; Real, J. A. *Angew. Chem., Int. Ed*. **2003**, *42*, 3760. (b) Molnár, G.; Niel, V.; Gaspar, A. B.; Real, J. A.; Zwick, A.; Bousseksou, A.; McGarvey, J. J. *J. Phys. Chem. B* **2002**, *106*, 9701. (c) Molnár, G.; Niel, V.; Real, J. A.; Dubrovinsky, L.; Bousseksou, A.; McGarvey, J. J. *J. Phys. Chem. B* **2003**, *107*, 3149. (d) Galet, A.; Muñoz, M. C.; Real, J. A. *Inorg. Chem*. **2006**, *45*, 4583. (e) Agustķ, G.; Muñoz, M. C.; Real, J. A. *Inorg. Chem*. **2008**, *47*, 2552. (f) Agustķ, G.; Muñoz, M. C.; Gaspar, A. B.; Real, J. A. *Inorg. Chem*. **2009**, *48*, 3371.
(11) (a) Verdaguer, M.; Bleuzen, A.; Marvaud, V.; Vaissermann, J.; Seuleiman, M.; Desplanches, C.; Scuiller, A.; Train, C.; Garde, R.; Gelly, G.; Lomenech, C.; Rosenman, I.; Veillet, P.; Cartier, C.; Villain, F. *Coord. Chem. Rev*. **1999**, *190−192*, 1023. (b) Beltran, L. M. C.; Long, J. R. *Acc. Chem. Res*. **2005**, *38*, 325. (c) Sokol, J. J.; Hee, A. G.; Long, J. R. *J. Am. Chem. Soc*. **2002**, *124*, 7656. (d) Choi, H. J.; Sokol, J. J.; Long, J. R. *Inorg. Chem*. **2004**, *43*, 1606.
(12) (a) Sato, O. *Acc. Chem. Res*. **2003**, *36*, 692. (b) Herrera, J. M.; Marvaud, V.; Verdaguer, M.; Marrot, J.; Kalisz, M.; Mathoniére, C. *Angew. Chem., Int. Ed*. **2004**, *43*, 5468. (c) Long, J.; Chamoreau, L. M.; Mathoniére, C.; Marvaud, V. *Inorg. Chem*. **2009**, *48*, 22. (d) Bleuzen, A.; Marvaud, V.; Mathoniere, C.; Sieklucka, B.; Verdaguer, M. *Inorg. Chem*. **2009**, *48*, 3453 and references therein
(13) (a) Lescouëzec, R.; Marilena Toma, L.; Vaissermann, J.; Verdaguer, M.; Delgado, F. S.; Ruiz-Pérez, C.; Lloret, F.; Julve, M. *Coord. Chem. Rev*. **2005**, *249*, 2691. (b) Rebilly, J. N.; Mallah, T. *Struct. Bond*. **2006**, *122*, 103.
(14) (a) Berlinguette, C. P.; Vaughn, D.; Cañada-Vilalta, C.; Galán-Mascarós, J. R.; Dunbar, K. R. *Angew. Chem., Int. Ed*. **2003**, *42*, 1523. (b) Schelter, E. J.; Prosvirin, A. V.; Dunbar, K. R. *J. Am. Chem. Soc*. **2004**, *126*, 15004. (c) Atanasov, M.; Comba, P.; Daul, C. A. *Inorg. Chem*. **2008**, *47*, 2449. (d) Atanasov, M.; Busche, C.; Comba, P.; Hallak, F. E.; Martin, B.; Rajaraman, G.; van Slageren, J.; Wadepohl, H. *Inorg. Chem*. **2008**, *47*, 8112.
(15) (a) Wang, S.; Zuo, J. L.; Zhou, H. C.; Song, Y.; Gao, S.; You, X. Z. *Eur. J. Inorg. Chem*. **2004**, *43*, 3681. (b) Song, Y.; Zhang, P.; Ren, X. M.; Shen, X. F.; Li, Y. Z.; You, X. Z. *J. Am. Chem. Soc*. **2005**, *127*, 3708.
(16) (a) Li, D. F.; Parkin, S.; Wang, G.; Yee, G. T.; Prosvirin, A. V.; Holmes, S. M. *Inorg. Chem*. **2005**, *44*, 4903. (b) Toma, L. M.; Lescouëzec, R.; Pasán, J.; Ruiz-Pérez, C.; Vaissermann, J.; Cano, J.; Carrasco, R.; Wernsdorfer, W.; Lloret, F.; Julve, M. *J. Am. Chem. Soc*. **2006**, *128*, 4842.
(17) Tregenna-Piggott, P. L. W.; Sheptyakov, D.; Keller, L.; Klokishner, S. L.; Ostrovsky, S. M.; Palii, A. V.; Reu, O. S.; Bendix, J.; Brock-Nannestad, T.; Pedersen, K.; Weihe, H.; Mutka, H. *Inorg. Chem*. **2009**, *48*, 128.
(18) Palii, A. V.; Ostrovsky, S. M.; Klokishner, S. I.; Tsukertlat, B. S.; Berlinguette, C. P.; Dunbar, K. R.; Galán-Mascarós, J. R. *J. Am. Chem. Soc*. **2004**, *126*, 16860.
(19) (a) Berlinguette, C. P.; Dragulescu-Andrasi, A.; Sieber, A.; Güdel, H. U.; Achim, C.; Dunbar, K. R. *J. Am. Chem. Soc*. **2005**, *127*, 6766. (b) Bonhommeau, S.; Molnár, G.; Galet, A.; Zwick, A.; Real, J. A.; McGarvey, J. J.; Bousseksou, A. *Angew. Chem., Int. Ed*. **2005**, *44*, 4069. (c) Nihei, M.; Ui, M.; Yokota, M.; Han, L.; Maeda, A.; Kishida, H.; Okamoto, H.; Oshio, H. *Angew. Chem., Int. Ed*. **2005**, *44*, 6484.
(20) (a) Sato, O.; Iyoda, T.; Fujishima, A.; Hashimoto, K. *Science* **1996**, *272*, 704. (b) Sato, O.; Kawakami, T.; Kimura, M.; Hishiya, S.; Kubo, S.; Einaga, Y. *J. Am. Chem. Soc*. **2004**, *126*, 13176. (c) Escax, V.; Champion, G.; Arrio, M. A.; Zacchigna, M.; Moulin, C. C. D.; Bleuzen, A. *Angew. Chem., Int. Ed*. **2005**, *44*, 4798. (d) Yamamoto, T.; Umemura, Y.; Sato, O.; Einaga, Y. *J. Am. Chem. Soc*. **2005**, *127*, 16065.
(21) (a) Moore, J. G.; Lochner, E. J.; Ramsey, C.; Dalal, N. S.; Stiegman, A. E. *Angew. Chem., Int. Ed*. **2003**, *42*, 2741.
(22) (a) Miyasaka, H.; Matsumoto, N.; Okawa, H.; Re, N.; Gallo, E.; Floriani, C. *Angew. Chem., Int. Ed. Engl*. **1995**, *34*, 1446. (b) Miyasaka, H.; Matsumoto, N.; Okawa, H.; Re, N.; Gallo, E.; Floriani, C. *J. Am. Chem. Soc*. **1996**, *118*, 981. (c) Miyasaka, H.; Ieda, H.; Matsumoto, N.; Re, N.; Crescenzi, R.; Floriani, C. *Inorg. Chem*. **1998**, *37*, 255. (d) Matsumoto, N.; Sunatsuki, Y.; Miyasaka, H.; Hashimoto, Y.; Luneau, D.; Tuchagues, J. P. *Angew. Chem., Int. Ed*. **1999**, *38*, 171. (e) Miyasaka, H.; Takahashi, H.; Madanbashi, H.; Sugiura, K.; Clérac, R.; Nojiri, H. *Inorg. Chem*. **2005**, *44*, 5969. (f) Miyasaka, H.; Julve, M.; Yamashita, M.; Clérac, R. *Inorg. Chem*. **2009**, *48*, 3420.
(23) (a) Zhang, Y. Z.; Gao, S.; Sun, H. L.; Su, G.; Wang, Z. M.; Zhang, S. W. *Chem. Commun*. **2004**, 1906. (b) Yeung, W. F.; Lau, P. H.; Wang, X. Y.; Gao, S.; Szeto, L.; Wong, W. T. *Inorg. Chem*. **2006**, *45*, 6756. (c) Jiang, L.; Choi, H. J.; Feng, X. L.; Lu, T. B.; Long, J. R. *Inorg. Chem*. **2007**, *46*, 2181.
(24) (a) Kim, J. L.; Yoo, H. S.; Koh, E. K.; Kim, H. C.; Hong, C. S. *Inorg. Chem*. **2007**, *46*, 8481. (b) Kim, J. L.; Yoo, H. S.; Koh, E. K.; Kim, H. C.; Hong, C. S. *Inorg. Chem*. **2007**, *46*, 10461. (c) Yoon, J. H.; Yoo, H. S.; Kim, H. C.; Yoon, S. W.; Suh, B. J.; Hong, C. S. *Inorg. Chem*. **2009**, *48*, 816. (d) Kim, J. L.; Kwak, H. Y.; Yoon, J. H.; Ryu, D. W.; Yoo, I. Y.; Yang, N.; Cho, B. K.; Park, J. G.; Lee, H.; Hong, C. S. *Inorg. Chem*. **2009**, *48*, 2956.
(25) Forum Issue on Molecular Magnetism: *Inorg. Chem*. **2009**, *48*, 3293.
(26) Miyasaka, H.; Saitoh, A.; Abe, S. *Coord. Chem. Rev*. **2007**, *251*, 2622 and references therein.
(27) Clemente-Leon, M.; Coronado, E.; Galan-Mascaros, J. R.; Gomez-Garcia, C. J.; Woike, T.; Clemente-Juan, J. M. *Inorg. Chem*. **2001**, *40*, 87.
(28) Silviu, N.; Floriana, T.; Catalin, M.; Christopher, A. M.; Narcis, A.; Winpenny Richard, E. P.; Marius, A. *Cryst. Growth Des*. **2007**, *7*, 1825.
(29) Yuan, M.; Zhao, F.; Zhang, W.; Pan, F.; Wang, Z. M.; Gao, S. *Chem.—Eur. J*. **2007**, *13*, 2937.
(30) (a) Koner, R.; Lin, H. H.; Wei, H. H.; Mohanta, S. *Inorg. Chem*. **2005**, *44*, 3524. (b) Madalan, A. M.; Avarvari, N.; Fourmigue, M.; Clerac, R.; Chibotaru, L. F.; Clima, S.; Andruh, M. *Inorg. Chem*. **2008**, *47*, 940.
(31) Gheorghe, R.; Cucos, P.; Andruh, M.; Costes, J. P.; Donnadieu, B.; Shova, S. *Chem.—Eur. J*. **2006**, *12*, 187.
(32) Nayak, M.; Koner, R.; Lin, H. H.; Flörke, U.; Wei, H. H.; Mohanta, S. *Inorg. Chem*. **2006**, *45*, 10764.

Schiff base manganese(III) building blocks and three cyanide-containing polycyanidemetalates, Scheme 1. X-ray diffraction analysis reveals the polynuclear cluster and two-dimensional coordination polymer nature for the former four compounds and latter two ones, respectively. Interestingly, investigation over the magnetic properties of the four clusters reveals some characteristics of metamagnet behavior at low temperatures due to the relatively strong intermolecular hydrogen-bonding interaction. The two complexes with a two-dimensional structure were revealed to exhibit three-dimensional antiferromagnetic ordering with typical metamagnetic behavior below 8.4 K for **5** and 11.5 K for **6**. To the best of our knowledge, there are very few examples of polynuclear clusters exhibiting 3D magnetic ordering relying on intermolecular interactions. This work may provide valuable information for the understanding and application of intermolecular hydrogen-bonding interactions in molecular magnetic materials.

Experimental Section

General Procedures and Materials. All of the reactions were carried out under an air atmosphere, and all chemicals and solvents used in the synthesis were reagent grade without further purification. $[Mg(1\text{-}CH_3im)_2(H_2O)_2Fe(CN)_5(1\text{-}CH_3im)]\cdot H_2O$ and $[Et_4N]_3[Fe(CN)_6]$ were prepared according to the literature methods.[33] $[Mn(L^1)(H_2O)_2]ClO_4$ and $[Mn(L^2)(H_2O)_2]ClO_4$ were available from our previous work.[34]

Caution! *KCN is hypertoxic and hazardous. Perchlorate salts of metal complexes with organic ligands are potentially explosive. They should be handled in small quantities with care.*

Preparation of Complexes 1−4. These four complexes were prepared using one similar procedure; therefore, only the synthesis of **1** was detailed as a typical representative. A red-brown CH_3CN and CH_3OH solution (10 mL, v/v = 2:1) of $[Mn(L^1)(H_2O)_2]ClO_4$ (0.2 mmol, 103.4 mg) was carefully layered onto a dark red aqueous solution (10 mL) of $[Mg(1\text{-}CH_3im)_2(H_2O)_2Fe(CN)_5(1\text{-}CH_3im)]\cdot H_2O$ (0.1 mmol, 51.1 mg). After the mixture stood for a few days in a dark box with the aim of avoiding decomposition of the cyanide-containing building block, dark brown crystals suitable for X-ray diffraction were obtained. They were collected by filtration, washed with cooled methanol−water, and dried at room temperature.

Complex 1. Yield: 51.2 mg, 48.3%. Anal. Calcd for $C_{63}H_{68}ClFeMn_3N_{13}O_{20.5}$(**1**): C, 47.55; H, 4.31; N, 11.44. Found: C, 47.35; H, 4.39; N, 11.32. Main IR bands (cm^{-1}): 2147 (s, νC≡N), 2119 (s, νC≡N), 1617 (vs, νC═N), 1095 (s, νCl═O).

Complex 2. Yield: 58.1 mg, 51.2%. Anal. Calcd for $C_{69}H_{84}ClFeMn_3N_{13}O_{22}$ (**2**): C, 48.65; H, 4.97; N, 10.69. Found: C, 48.71; H, 5.00; N, 10.48. Main IR bands (cm^{-1}): 2146 (s, νC≡N), 2116 (s, νC≡N), 1618 (vs, νC═N), 1093 (s, νCl═O).

Complex 3. Yield: 83.4 mg, 52.4%. Anal. Calcd for $C_{138}H_{168}Fe_2Mn_6N_{24}O_{36}$ (**3**): C, 52.12; H, 5.32; N, 10.57. Found: C, 52.21; H, 5.41; N, 10.52. Main IR bands (cm^{-1}): 2149 (s, νC≡N), 2121 (s, νC≡N), 1600 (vs, νC═N).

Complex 4. Yield: 89.3 mg, 56.3%. Anal. Calcd for $C_{138}H_{168}Cr_2Mn_6N_{24}O_{36}$ (**4**): C, 52.24; H, 5.34; N, 10.60. Found: C, 50.13; H, 5.46; N, 10.73. Main IR bands (cm^{-1}): 2152 (s, νC≡N), 2114 (s, νC≡N), 1613 (vs, νC═N).

Preparation of Complexes 5 and 6. With the employment of the above-mentioned procedure used to prepare complex **1** using $[Et_4N]_3[Fe(CN)_6]$ or $K_3[Cr(CN)_6]$ instead of $[Mg(1\text{-}CH_3im)_2(H_2O)_2FeCN_5(1\text{-}CH_3im)]\cdot H_2O$ as a starting material, complexes **5** and **6** were synthesized.

(33) (a) Johnson, C. R.; Jones, C. M.; Asher, S. A.; Abola, J. E. *Inorg. Chem.* **1991**, *30*, 2120. (b) Mascharak, P. K. *Inorg. Chem.* **1986**, *25*, 247.

(34) Ni, Z. H.; Zheng, L.; Zhang, L. F.; Cui, A. L.; Ni, W. W.; Zhao, C. C.; Kou, H. Z. *Eur. J. Inorg. Chem.* **2007**, 1245.

Scheme 1

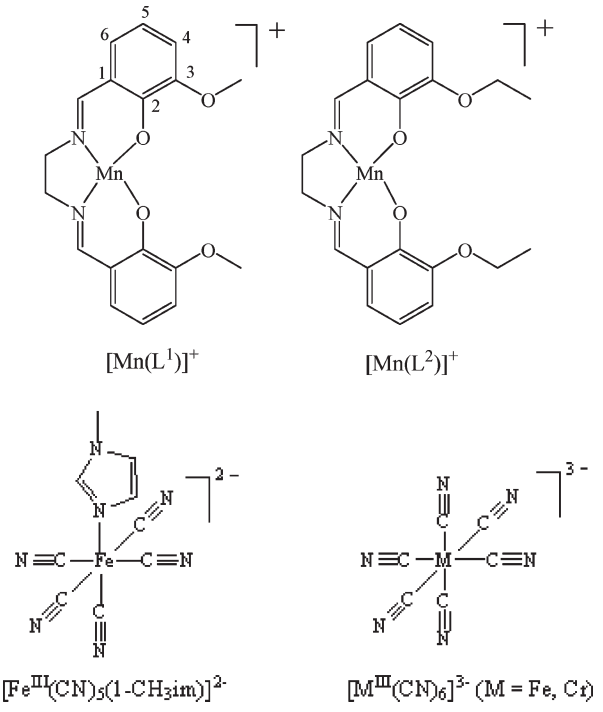

Complex 5. Yield: 53.2 mg, 46.7%. Anal. Calcd for $C_{48}H_{53}FeMn_2N_{12}O_{11}$ (**5**): C, 50.58; H, 4.69; N, 14.75. Found: C, 50.51; H, 4.62; N, 14.89. Main IR bands (cm^{-1}): 2152 (s, νC≡N), 2124 (s, νC≡N), 1605 (vs, νC═N).

Complex 6. Yield: 59.9 mg, 54.3%. Anal. Calcd for $C_{46}H_{44.50}CrKMn_2N_{11.5}O_9$ (**6**): C, 50.07; H, 4.07; N, 14.60. Found: C, 50.02; H, 4.06; N, 14.68. Main IR bands (cm^{-1}): 2154 (s, νC≡N), 2119 (s, νC≡N), 1680 (s, νN═O), 1611 (vs, νC═N).

Physical Measurements. Elemental analyses of carbon, hydrogen, and nitrogen were carried out with an Elementary Vario El. Infrared spectra were measured by using KBr disks with a Shimadzu FTIR-8600 spectrophotometer. Magnetic susceptibility measurements were obtained with a Quantum Design SQUID MPMS-XL magnetometer. The dc measurements were collected from 2 to 300 K and from 0 to 50 kOe, and the ac measurements were performed at various frequencies by using a Maglab 2000 magnetometer. All of the experimental susceptibilities were corrected for the diamagnetism of the constituent atoms (Pascal's tables).

X-Ray Data Collection and Structure Refinement. Single crystals of all of the complexes for X-ray diffraction analyses with suitable dimensions were mounted on a glass rod, and the crystal data were collected on a Bruker SMART CCD diffractometer with a Mo Kα sealed tube (λ = 0.71073 Å) at 293 K, using the ω scan mode. The structures were solved using the direct method and expanded using Fourier difference techniques with the SHELXTL-97 program package. The non-hydrogen atoms were refined anisotropically, while hydrogen atoms were introduced as fixed contributors. All of the nonhydrogen atoms, except the disordered ones, were refined with anisotropic displacement coefficients. For the disordered contents, the balance anion ClO_4^- and the free water molecules in **1**, the solvent acetonitrile molecules in **5**, the partially occupied atoms were refined with isotropic displacement parameters. Hydrogen atoms were assigned isotropic displacement coefficients $U(H) = 1.2U(C)$ or $1.5U(C)$, and their coordinates were allowed to ride on respective carbons using SHELXL97, except some H atoms of the solvent molecules, which were refined isotropically with fixed U values. The DFIX command was used to rationalize

Table 1. Details of the Crystal Parameters, Data Collection, and Refinement for Complexes **1**−**6**

	1	2	3	4	5	6
chemical formula	$C_{63}H_{68}ClFeMn_3N_{13}O_{20.5}$	$C_{69}H_{84}ClFeMn_3N_{13}O_{22}$	$C_{138}H_{168}Fe_2Mn_6N_{24}O_{36}$	$C_{138}H_{168}Cr_2Mn_6N_{24}O_{36}$	$C_{48}H_{53}FeMn_2N_{12}O_{11}$	$C_{46}H_{44.5}CrKMn_2N_{11.5}O_9$
fw	1591.42	1703.61	3180.30	3172.60	1139.75	1103.41
cryst syst	monoclinic	monoclinic	rhombohedral	rhombohedral	monoclinic	monoclinic
space group	P2(1)/c	*C*2/*c*	$R\bar{3}$	$R\bar{3}$	P2(1)/c	P2(1)/c
a/Å	14.589(3)	45.143(7)	22.428(3)	22.4937(13)	13.7503(16)	16.061(3)
b/Å	12.969(3)	13.5963(19)	22.428(3)	22.4937(13)	12.4710(14)	12.552(3)
c/Å	40.134(9	29.452(6	24.836(5)	25.036(2)	15.7795(17)	27.579(6)
α/deg	90	90	90	90	90	90
β/deg	99.80	116.588(5)	90	90	103.158(2)	101.881(4)
γ/deg	90	90	120	120	90	90
V/Å^3	7483(3)	16165(5)	10819(3)	10970.4(13)	2634.8(5)	5441(2)
Z	4	8	3	3	2	4
F(000)	3276	7064	4962	4950	1178	2264
θ/deg	1.65−25.01	1.58−25.01	1.82−25.01	1.81−25.01	2.10−25.01	1.79−25.01
GOF	1.003	1.012	1.04	1.033	1.003	1.032
R_1 [$I > 2\sigma(I)$]	0.0798	0.0747	0.0563	0.0548	0.0558	0.08
wR_2 (all data)	0.2365	0.2226	0.1602	0.1754	0.1311	0.2625

the bond parameter. Details of the crystal parameters, data collection, and refinement are summarized in Table 1.

Results and Discussion

Synthesis and General Characterization. Despite the wide range of employment of traditional cyanide-containing building blocks, $K_3[Fe^{III}(CN)_6]$, in synthesizing the cyanide-bridged heterometallic complexes, reports on the paramagnetic polycyanidemetalates containing five cyanide groups with the unit formula of $[Fe^{III}(L)(CN)_5]^{n-}$ (L is a monodentate terminal ligand) still remain rare.[35] Due to the different number of charges and cyanide groups together with the different symmetries and steric effects associated with the ancillary ligand, polycyanidemetalates $[Fe(L)(CN)_5]^{n-}$ will lead to heterometallic complexes with different molecular structures from those of $K_3[Fe(CN)_6]$. On the other hand, the manganese(III) compounds prepared from bicompartmental Schiff base ligands (H_2L^1 or H_2L^2) are able to form supramolecular structures via their O_4 compartment, which are therefore selected as another precursor for the directional assembly of cyanide-bridged heterometallic complexes in the present work.

By reacting $[Mg(1\text{-}CH_3im)_2(H_2O)_2Fe(CN)_5(1\text{-}CH_3im)]\cdot H_2O$ with $[Mn(L^1)(H_2O)_2]ClO_4$ or $[Mn(L^2)(H_2O)_2]ClO_4$ in a molar ratio of 1:2, two heterometallic tetranuclear cyanide-bridged complexes, $\{[Mn(L^1)(H_2O)]_3[Fe(CN)_5(1\text{-}CH_3im)]\}ClO_4\cdot 1.5H_2O$ (**1**) and $\{[Mn(L^2)(H_2O)]_3[Fe(CN)_5(1\text{-}CH_3im)]\}ClO_4\cdot 3H_2O$ (**2**), consisting of $\{[Mn(L)(H_2O)]_3[FeCN_5(1\text{-}CH_3im)]\}^+$ (L = L^1 or L^2) and $[ClO_4]^-$ balance anions, were obtained. With the use of $K_3[Fe(CN)_6]$ instead of $[Mg(1\text{-}CH_3im)_2(H_2O)_2Fe(CN)_5(1\text{-}CH_3im)]\cdot H_2O$ as a starting material to react with $[Mn(L^2)(H_2O)_2]ClO_4$, heterometallic heptanuclear cyanide-bridged cage-shaped complex $\{[Mn(L^2)(H_2O)]_6[Fe(CN)_6]\}[Fe(CN)_6]\cdot 6CH_3OH$ (**3**) was synthesized. In a similar manner, an analogous heterometallic heptanuclear cyanide-bridged cage-shaped compound, $\{[Mn(L^2)(H_2O)]_6[Cr(CN)_6]\}[Cr(CN)_6]\cdot 6CH_3OH$ (**4**), was obtained with $K_3[Cr(CN)_6]$ as a starting material. Interestingly, the T-like tetranuclear structure for **1** and **2** and the heptanuclear cage-shaped structure for **3** and **4** can be linked into one-dimensional ladder-like double-chain structures and three-dimensional networks, depending on intermolecular hydrogen-bond interactions. Two cyanide-bridged two-dimensional $M^{III}-Mn^{III}$ coordination polymers, $\{[H_3O][Mn(L^1)]_2[Fe(CN)_6]\}\cdot 2DMF$ (**5**) and $\{K[Mn(L^1)]_2[Cr(CN)_6]\}\cdot 1.5CH_3CN\cdot CH_3OH$ (**6**), were synthesized by treating $[Et_4N)_3[Fe(CN)_6]$ or $K_3[Cr(CN)_6]$ with $[Mn(L^1)(H_2O)_2]ClO_4$, revealing the effect of the number of charges and cyanide groups of polycyanidemetlates as well as the position and size of the substituted group at the Schiff base ligand on the structure of cyanide-bridged heterometallic complexes. It is worth noting that the two 2D $M^{III}-Mn^{III}$ coordination polymers **5** and **6** are structurally similar to another $Fe^{III}-Mn^{III}$ compound reported previously by Miyasaka and co-workers.[22b]

All of the cyanide-bridged heterometallic complexes, **1**−**6**, have been characterized by IR spectroscopy. In the IR spectra of **1**−**6**, two sharp peaks due to the cyanide-stretching vibration were observed at about 2120 and 2150 cm^{-1}, indicating the presence of bridging and nonbridging cyanide ligands in these complexes. For **1** and **2**, the strong broad peak centered at 1090 cm^{-1} is attributed to the free ClO_4^- anions.[22b]

Crystal Structures of Complexes 1−**4**. Some important structural parameters for complexes **1**−**4** are collected in Table 2. The cationic structure of **1** and its one-dimensional ladder-like double-chain structure formed depending on intermolecular hydrogen bonding are shown in Figures 1 and 2, respectively. The corresponding diagrams for **2** are given in Figures S1 and S2 (Supporting Information).

As shown in Figure 1, in compound **1**, $[Fe(1\text{-}CH_3im)CN_5]^{2-}$, acting as a *mer*-$\mu_3$-coordinating-donor building block, binds three $[Mn(L^1)(H_2O)]^+$ moieties together with an additional disordered ClO_4^- as a balance anion, forming a neutral heterometallic tetranuclear cyanide-bridged complex. This is also true for **2**. In both **1** and **2**, each $[Mn(L^1/L^2)(H_2O)]$ moiety has an elongated octahedral geometry with a Jahn−Teller distortion along the $(H_2O)-Mn-N_{cyanide}$ axis, which can be testified to by the coordination parameter around the Mn(III) ion

(35) (a) Culp, J. T.; Park, J. H.; Meisel, M. W.; Talham, D. R. *Inorg. Chem.* **2003**, *42*, 2842. (b) Ni, W. W.; Ni, Z. H.; Cui, A. L.; Liang, X.; Kou, H. Z. *Inorg. Chem.* **2007**, *46*, 22. (c) Zhao, C. C.; Ni, W. W.; Tao, J.; Cui, A. L.; Kou, H. Z. *CrystEngComm*. **2009**, *11*, 632.

Table 2. Selected Bond Lengths (Å) and Angles (deg) for Complexes **1**−**4**

	1	**2**		**3** (M = Fe)	**4** (M = Cr)
Mn(1)−N(1)	2.268(6)	2.253(6)	M(1)−C(1)	1.944(4)	2.069(4)
Mn(2)−N(2)	2.244(6)	2.245(6)	M(2)−C(22)	1.946(5)	2.078(5)
Mn(3)−N(3)	2.264(5)	2.252(6)	Mn(1)−N(1)	2.299(4)	2.302(3)
Mn(1)−N(8)	1.966(6)	1.970(6)	Mn(1)−N(2)	1.975(3)	1.984(3)
Mn(1)−N(9)	1.975(5)	1.987(6)	Mn(1)−N(3)	1.984(3)	1.981(3)
Fe(1)−N(6)	1.980(6)	1.982(6)	Mn(1)−O(1)	1.871(3)	1.864(3)
Fe(1)−C(1)	1.925(7)	1.923(7)	Mn(1)−O(2)	1.857(3)	1.869(3)
Fe(1)−C(2)	1.921(7)	1.956(7)	Mn(1)−O(5)	2.322(3)	2.303(3)
Fe(1)−C(3)	1.918(7)	1.922(7)			
C(1)−N(1)−Mn(1)	144.7(5)	146.1(5)	C(1)−N(1)−Mn(1)	152.0(3)	151.3(3)
C(2)−N(2)−Mn(2)	147.5(5)	157.2(5)	N(1)−C(1)−Fe(1)	177.8(3)	176.3(3)
C(3)−N(3)−Mn(3)	142.5(5)	149.0(5)	N(4)−C(22)−Fe(2)	178.0(5)	177.4(5)

(Table 2). The $Mn-N_{cyanide}$ bond lengths are almost equal to each other and in good agreement with the corresponding distance in $[Mn(salen)(EtOH)]_3[M(CN)_6]$ (M = Fe, Cr) reported previously.[22e] The Mn−N≡C angles in **1** are close to each other with values of 144.7(5), 147.5(5), and 142.5(5)°, while the Mn(2)−N(2)≡C(2) angle, 157.2(5)°, is slightly bigger than the other two Mn−N≡C angles with values of 146.1(5) and 149.0(5)° in **2**. It is worth noting that almost all of the Mn−N≡C angles for these two complexes are smaller than those in $[Mn(salen)(EtOH)]_3[Fe(CN)_6]$.[22e] The intramolecular Mn−Fe distances through bridging cyanides are very close to each other with values of 5.034, 5.054, and 5.088 Å for **1** and 5.109, 5.175, and 5.105 Å for **2**, all of which are slightly longer than the shortest intermolecular metal−metal separations of 4.678 and 4.823 Å in these two complexes.

Due to the excellent encapsulation ability of the O_4 compartment for the H_2O molecule, a one-dimensional chain is formed depending on the relatively strong hydrogen-bond interactions between the O_{H_2O} atoms and the O atoms of the Schiff-base ligand, Table S1 (Supporting Information). Additionally, two chains can be linked together by the same type of hydrogen-bond interaction, forming a ladder-like double-chain structure.

The asymmetric cationic unit and heptanuclear cationic crystal structure of complex **3** and its three-dimensional supramolecular structure formed depending on intermolecular hydrogen-bond interactions, which are just the same as those in the above two complexes, **1** and **2**, and are depicted in Figures 3 and 4, respectively. Those for **4** are given in Figures S3 and S4 (Supporting Information). Complexes **3** and **4**, comprising a heptanuclear $M^{III}Mn^{III}_6$ [M = Fe (**3**), Cr (**4**)] cation with $[M(CN)_6]^{3-}$ acting as a counteranion, are isostructural. The coordinated $[M(CN)_6]^{3-}$ unit locates in the center of an octahedron formed by six $[Mn(L^2)(H_2O)]^+$ units, similar to that in other cyanide-bridged M−Mn (M = Fe, Cr) complexes also containing a MMn_6 core.[36,37] The Mn−N and Mn−O bond lengths listed in Table 2 indicate that the coordination sphere of the Mn(III) ion is a distorted octahedron. All of the bond parameters for **3** and **4** are basically consistent with those in the reported complexes.[36,37] The Mn−N≡C angle is 152.0(3) for **3** and 151.3(3)° for **4**, respectively, demonstrating the significant deviation of these three atoms from a linear configuration. These angles are also comparable to those in other cyanide-bridged heptanuclear MMn_6 complexes with similar structures to those of **3** and **4**[36] but slightly smaller than those found in $[\{(talen^{tBu}2)(Mn(MeOH))_3\}_2\{Fe(CN)_6\}][Fe(CN)_6]$ and $[\{(talen^{tBu2})Mn_3\}_2\{Cr(CN)_6\}(MeOH)_3(CH_3CN)_2](BPh_4)_3\cdot 4CH_3CN\cdot 2Et_2O$.[37] The distance between the central metal ion and Mn ion bridged by a cyanide group, 5.221 Å for **3** and 5.322 Å for **4**, is slightly longer than the shortest intermolecular metal−metal distance with values of 5.179 Å and 5.068 Å for **3** and **4**, respectively. Similar to that in **1** and **2**, a hydrogen-bond interaction between the O_{water} atoms and the $O_{Schiff\text{-}base}$ atoms can also be found in **3** and **4**, linking the cage-shaped heptanuclear cationic units MMn_6 into an infinite three-dimensional network.

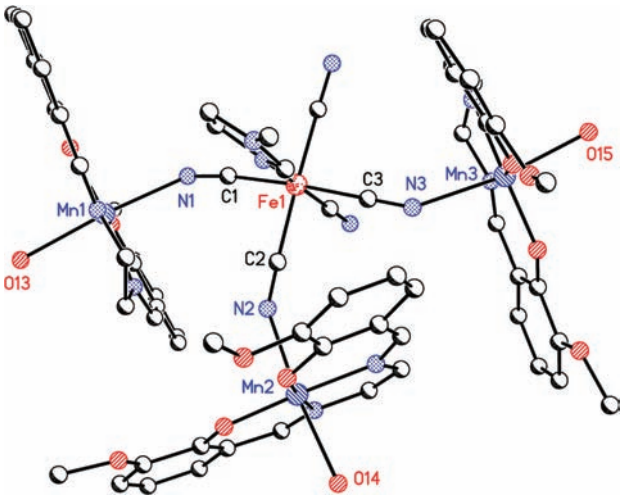

Figure 1. Cationic crystal structure of complex **1**. All of the H atoms, the solvent molecule, and the balanced ClO_4^- have been omitted for clarity.

Crystal Structures of Complexes 5 and 6. The selected bond lengths and angles for **5** and **6** are shown in Table S2 (Supporting Information). For **5**, its trinuclear anionic structure and two-dimensional network are shown in Figures 5 and 6, respectively. Those for **6** together with its cell packing diagram are given in Figures S5, S6, and S7 (Supporting Information). In **5** and **6**, whose structures are similar to that of another cyanide-bridged

(36) (a) Shen, X. P.; Li, B. L.; Zou, J.; Zou, J. Z.; Xu, Z. *Trans. Met. Chem.* **2002**, *27*, 372. (b) Shen, X. P.; Li, B. L.; Zou, J.; Zou, J. Z.; Hu, H. M.; Xu, Z. *J. Mol. Struct.* **2003**, *657*, 325.

(37) (a) Glaser, T.; Heidemeier, M.; Weyhermüller, T.; Hoffmann, R. D.; Rupp, H.; Müller, P. *Angew. Chem., Int. Ed.* **2006**, *45*, 6033. (b) Glaser, T.; Heidemeier, M.; Krickemeyer, E.; Bögge, H.; Stammler, A.; Fröhlich, R.; Bill, E.; Schnack, J. *Inorg. Chem.* **2009**, *48*, 607.

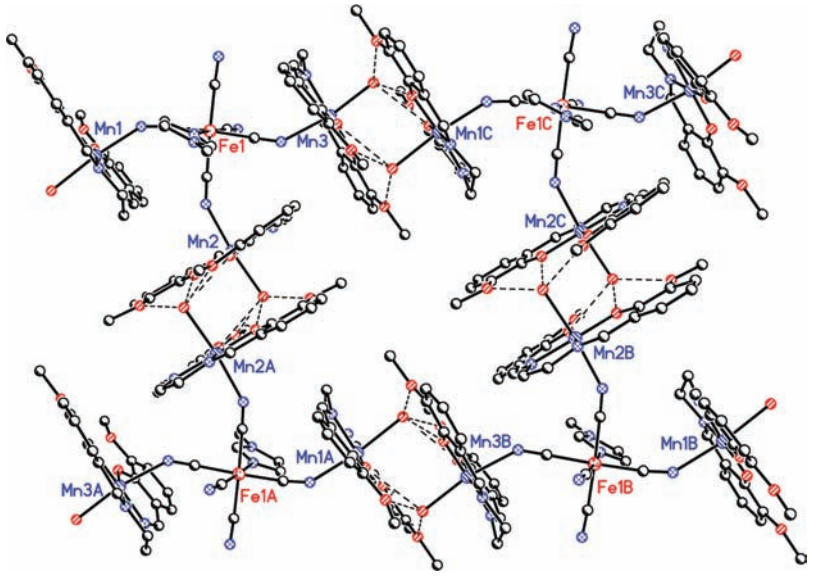

Figure 2. One-dimensional double-chain structure of complex **1** formed by intermolecular hydrogen-bond interactions. All of the H atoms except those used to form hydrogen bonds, solvent molecules, and the balance ClO_4^- have been omitted for clarity.

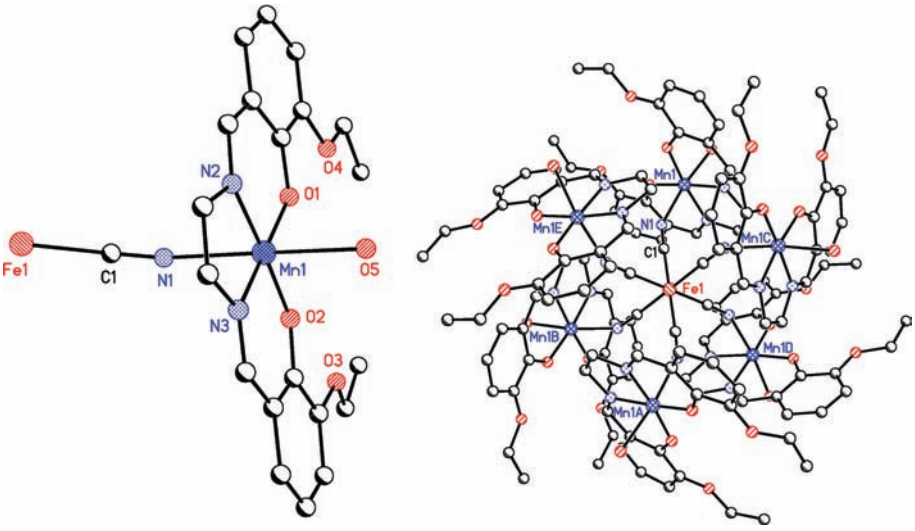

Figure 3. Asymmetric cationic unit of complex **3** (left) and its heptanuclear cationic crystal structure (right). All of the H atoms, the solvent molecules, and the balanced $[Fe(CN)_6]^{3-}$ have been omitted for clarity.

Fe−Mn complex, K[Mn(3-MeOsalen)]$_2$[Fe(CN)$_6$]·DMF reported by Miyasaka et al.,[22a,b] the coordination sphere for both Fe(Cr) and Mn ions is octahedral, among which, the one for the Mn ion is slightly distorted due to the typical Jahn−Teller effect. The $[M(CN)_6]^{3-}$ unit as a tetradentate ligand is coordinated to four $[Mn(L^1)(H_2O)]$ units through its four cyanide groups located in trans positions to each other, resulting in a layered 2D network containing a repeating cyclic $[(-Mn-NC-M-CN-)]_4$ unit with the solvent molecules filled in the interlayer space. The 24-membered macrocycle formed by four $[-Mn-NC-M-CN-]_4$ units is separated by a KO_8 unit in **6**, the same as that in K[Mn(3-MeOsalen)]$_2$[Fe(CN)$_6$]·DMF,[22a,b] while in **5**, it is separated by a $[H_3O]^+$ linked to two O_4 units through hydrogen-bond interactions. Two types of Mn−N≡C bond angles with obvious differences were found in these two complexes, at distances of 137.7(4) and 170.9(4)° for **5**, which are very close to the values of 137.2(4) and 169.5(5)° in the above-mentioned complex.[22b] For complex **6**, they are about 140 and 163°, respectively.

Magnetic Properties of Complexes 1 and 2. The temperature dependences of the $\chi_m T$ product per $Fe^{III}Mn^{III}_3$ unit for **1** and **2** measured from 2 to 300 K under an applied magnetic field of 2000 Oe are shown in Figure 7 and Figure S8 (Supporting Information). The $\chi_m T$ value at room temperature is 9.11 emu K mol^{-1} for **1** and 9.08 emu K mol^{-1} for **2**, which is slightly lower than the spin-only value of 9.375 emu K mol^{-1} for three uncoupled high-spin Mn(III)'s ($S = 2$) and one low-spin Fe(III) ($S = 1/2$) on the basis of $g = 2.00$. With a decrease in the temperature, the $\chi_m T$ for these two complexes maintains a nearly constant value until about 50 K, then starts to increase smoothly, reaches a highest value of about 9.58 emu K mol^{-1} for **1** and 9.92 emu K mol^{-1} for **2**, and then decreases rapidly to a lowest value of about 1.39 emu K mol^{-1} for **1** and 0.83 emu K mol^{-1} for **2** at 2 K. The magnetic susceptibilities of **1** and **2** conform well to

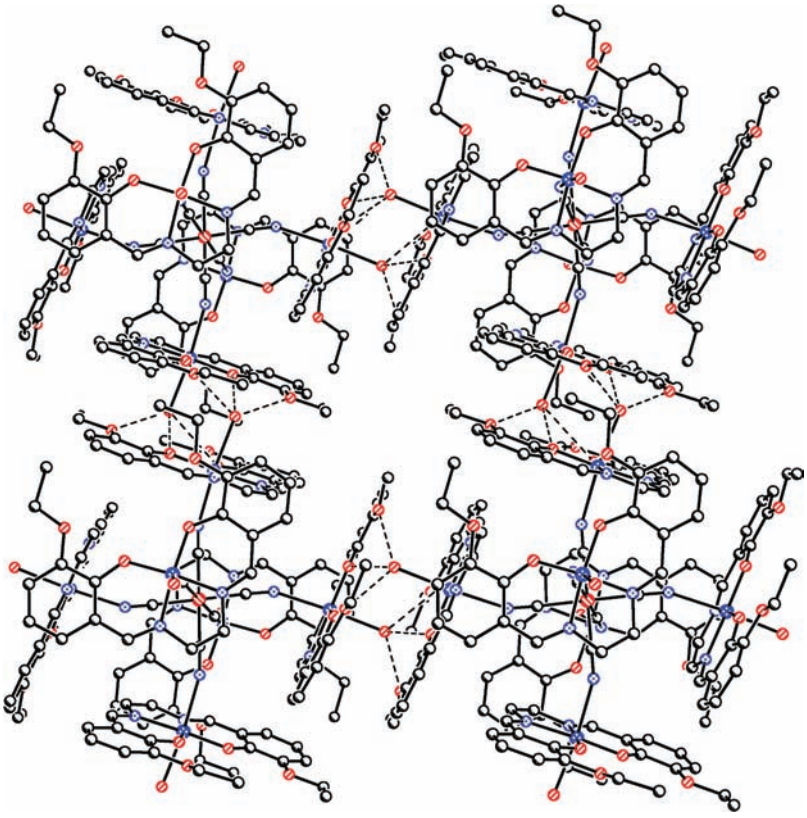

Figure 4. The 3D supermolecular structure of complex **3** formed by intermolecular hydrogen-bond interactions. All of the H atoms except those used to form hydrogen bonds, solvent molecules, and the balance $[Fe(CN)_6]^{3-}$ have been omitted for clarity.

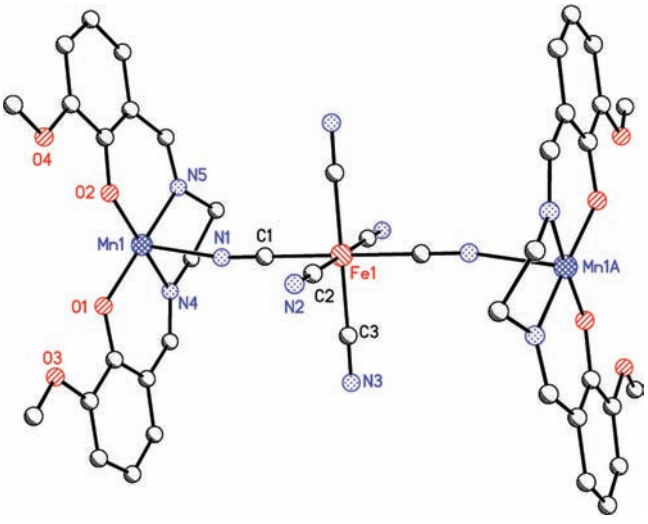

Figure 5. Anionic trinuclear structure of complex **5**. All of the H atoms, the solvent molecules, and the balanced $[H_3O]^+$ cation have been omitted for clarity.

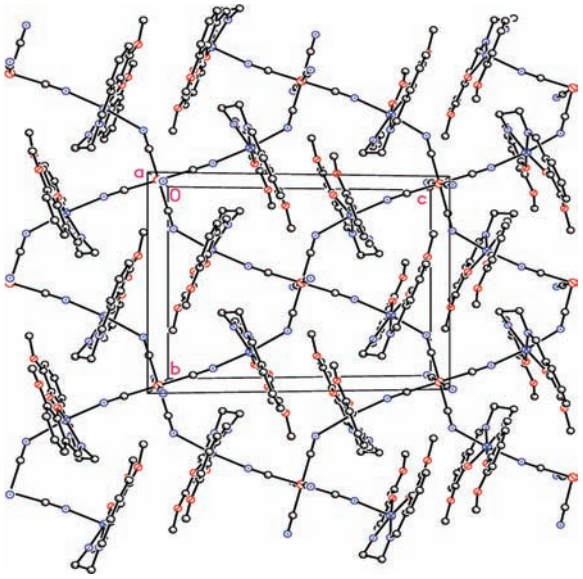

Figure 6. Anionic 2D network structure of complex **5**. All of the H atoms, the solvent molecules, and the balanced $[H_3O]^+$ cation have been omitted for clarity.

Curie−Weiss law in the range of 10−300 K and give a positive Weiss constant $\theta = 1.66$ K and a Curie constant $C = 8.87$ emu K mol^{-1} for **1** and $\theta = 1.97$ K and $C = 9.02$ emu K mol^{-1} for **2**. On the basis of these above-discussed data, the overall ferromagnetic magnetic coupling between Fe(III) and Mn(III) ions through cyanide bridges in **1** and **2** can be concluded.

In view of the situation that the three Mn−N≡C−Fe bridges are structurally independent in these two complexes, in which the coordination environments of the three Mn(III) ions are not completely the same as each other, with the Mn−C≡N angles locating in a narrow range of 142.5(5)−147.5(5)° for **1** and 146.1(5)−157.2(5)° for **2** and the Mn−N_{CN} bond lengths distributing also in a very narrow range of 2.244(6)−2.264(5) Å, the simulation of the magnetic susceptibilities should be based on $J_1 \neq J_2 \neq J_3$, where J_1, J_2, and J_3 represent the Mn(1)···Fe(1), Mn(2)···Fe(1), and Mn(3)···Fe(1) interactions

through cyanide bridges, respectively. Evaluating the exchange coupling between the Fe(III) and Mn(III) bridged by a cyanide group is carried out, and the magnetic susceptibilities of these two complexes are simulated by the MAGPACK program. Considering that the effects resulted from the zero-field splitting (ZFS) of the Mn(III) ion and the intermolecular interactions are relatively small and can therefore be safely neglected, the data of the experimental $\chi_m T$ value of 20−300 K was used for fitting.

The best-fit parameters obtained are $J_1 = 1.24$, $J_2 = 1.58$, $J_3 = 0.71$ cm^{-1}, $g = 2.01(3)$, and $R = 1.21 \times 10^{-5}$ for **1** and $J_1 = 1.25$, $J_2 = 0.63$, $J_3 = 1.13$ cm^{-1}, $g = 2.10(4)$ cm^{-1}, and $R = 1.47 \times 10^{-5}$ for **2**. On the basis of the above-obtained data and the spin ground state (11/2 for **1** and **2**), a primary conclusion can be derived that the overall magnetic coupling between the Fe(III) ion and Mn(III) ion through a cyanide bridge in both **1** and **2** is ferromagnetic, which is also consistent with the previous findings that general ferromagnetic coupling exists between the $Fe^{III}-Mn^{III}$ bridged by a cyanide group when the Mn−N≡C angle is around 150°.[22e]

It is noteworthy that, in the case that all of the data even below 10 K were also employed for simulation, no satisfactory result could be obtained. As described above, there exist abundant hydrogen-bond interactions between the asymmetry units of complexes **1** and **2**, Table S1 (Supporting Information), which in turn results in infinite structures for both **1** and **2**. In addition, in comparison with other intermolecular interactions, which are usually very weak, hydrogen-bond interaction usually results in relatively strong magnetic exchange coupling, as revealed for other transition metal complexes.[28,38] As a result, the failed simulation for the magnetic susceptibility at low temperatures can be attributed to the neglect of the ZFS effect and the intermolecular hydrogen interactions.

The field-dependent magnetization was measured up to 50 kOe at 2 K for **1** and **2**, Figure S9 (Supporting Information). The curves have a sigmoid shape, typical of metamagnetic behavior: The magnetization first increases slowly with increasing magnetic field until 20 kOe is reached due to the relatively strong intermolecular hydrogen-bond interaction, then increases abruptly for a phase transition at about 20 kOe, and finally attains a highest value about 7.45 Nβ for **1** and 7.69 Nβ for **2** at 50 kOe. To confirm the magnetic phase transition at low temperatures, the field cooled magnetization (FCM) curves were measured under different magnetic fields in the range of 2−30 K (inset of Figure 7 and Figure S8 (Supporting Information)). Below 20 kOe, the FCM curves show a peak at 6.0 K for **1** and 6.1 K for **2**, which can be considered as the phase transition temperature. The absence of a peak at 30 kOe, actually the value of the critical field (H_c) needed to overcome the intermolecular antiferromagnetic interaction, confirms the metamagnetic behavior of these two complexes at low

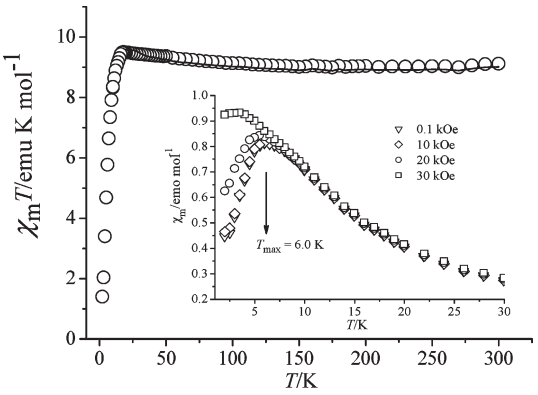

Figure 7. Temperature dependence of $\chi_m T$ (the solid line represents the best fit on the basis of the parameters discussed in the text) for complex **1**. Inset: Field-cooled magnetization of complex **1** in applied fields of 0.1, 10, 20, and 30 kOe.

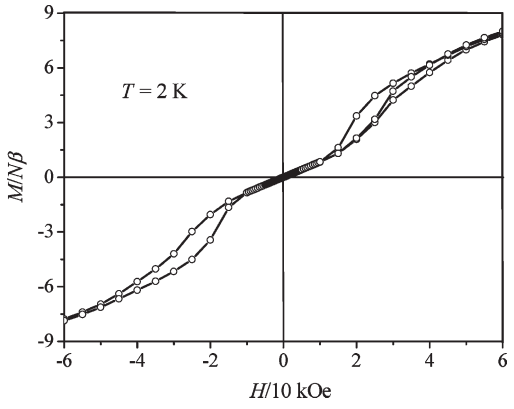

Figure 8. Magnetic hysteresis loop for complex **1** at 2 K.

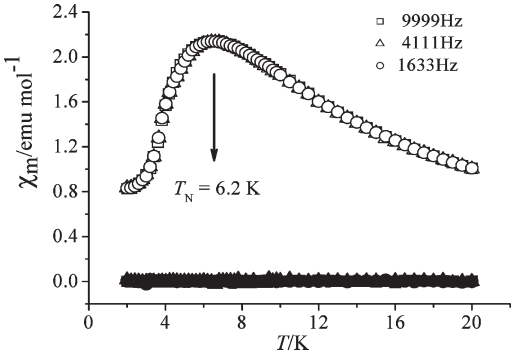

Figure 9. Temperature dependence of ac magnetization of complex **2** in a zero-static field and an ac field of 3 Oe at frequencies of 1633, 4111, and 9999 Hz. The white and black marks represent the real and imaginary part of the ac magnetic measurement, respectively.

temperatures. This is further supported by their hysteresis loops measured at 2 K, Figure 8 and Figure S10 (Supporting Information). The ac magnetic susceptibility measurement for **1** and **2** was performed in a 3.0 Oe ac field oscillating at 1633, 4111, and 9999 Hz with a zero dc field, Figure S11 (Supporting Information) and Figure 9. Observation of the peak at about 6.0 K in these two figures also indicates the three-dimensional magnetic ordering for these two complexes below 6.0 K.

Magnetic Properties of Complexes 3 and 4. The temperature dependence of magnetic susceptibilities for **3** and

(38) (a) Plass, W.; Pahlmann, A.; Rautengarten, J. *Angew. Chem., Int. Ed.* **2001**, *40*, 4207. (b) Desplanches, C.; Ruiz, E.; Rodrgkuez-Fortea, A.; Alvarez, S. *J. Am. Chem. Soc.* **2002**, *124*, 5197. (c) Tang, J. K.; Coster, J. S.; Golobi, A.; Kozlevar, B.; Robertazzi, A.; Vargiu, A. V.; Gamez, P.; Reedijk, J. *Inorg. Chem.* **2009**, *48*, 5473.

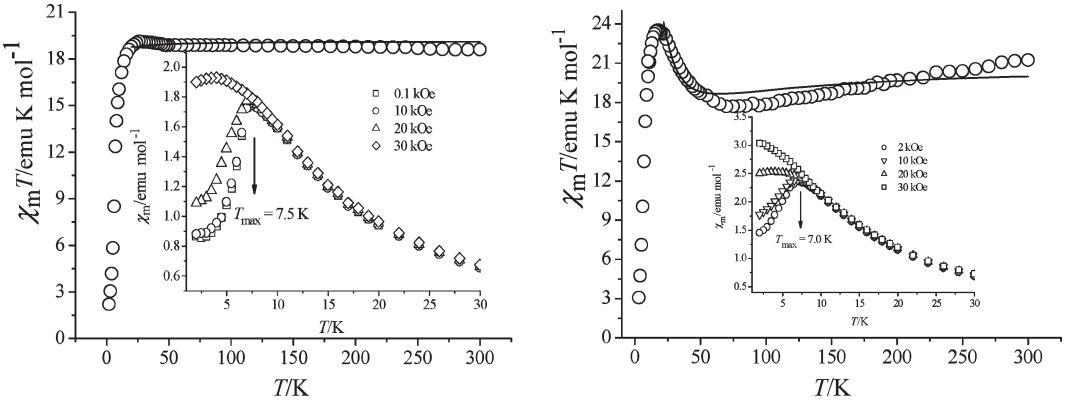

Figure 10. Temperature dependence of $\chi_m T$ for complexes **3** (left) and **4** (right). Inset: Field-cooled magnetization of complex **3** in applied fields of 0.1, 10, 20, and 30 kOe. Complex **4**: 2, 10, 20, and 30 kOe.

4 measured in the range of 2−300 K under an external magnetic field of 2000 Oe is illustrated in Figure 10. The room-temperature values of $\chi_m T$ for these two complexes are 18.90 and 21.45 emu K mol^{-1}, basically consistent with the spin-only values of 19.75 and 21.75 emu K mol^{-1} for six high-spin Mn(III)'s (S = 2) and two low-spin Fe(III)'s (S = 1/2) or Cr(III) (S = 3/2). With the temperature lowering, the $\chi_m T$ value for **3** increases very slowly until about 30 K, then decreases rapidly to 1.70 emu K mol^{-1} at 2 K. For complex **4**, the $\chi_m T$ value decreases smoothly from 300 K to about 60 K, then increases rapidly to a value of 23.62 emu K mol^{-1} at 15 K, and then decreases again with a high speed to a minimum of 3.1 emu K mol^{-1} at 2 K. The whole changing tendency of the $\chi_m T$ for these two complexes is very similar to that of the other two heptanuclear MMn_6 (M = Fe, Cr) clusters reported previously.[36] Their magnetic susceptibilities obey the Curie−Weiss law in the range of 20−300 K for **3** and 50−300 K for **6** and afford positive and negative Weiss constants, respectively, primarily indicating the ferromagnetic coupling in **3** and antiferromagnetic coupling in **4** between the central metal ion and Mn(III) ion bridged by a cyanide group.

The simulation of the magnetic susceptibilities for **3** and **4** was also carried out by using the MAGPACK program using the data for 20−300 K. The obtained fitting parameters are J = 0.47 cm^{-1}, g = 1.99(7), and $R = 3.55 \times 10^{-5}$ for **3** and J = −3.49 cm^{-1}, g = 2.03(7), and $R = 6.19 \times 10^{-4}$ for **4**, respectively. These coupling J values are comparable to those found in other cyanide-bridged $M^{III}Mn^{III}$ complexes.[11d,22e,39−41] The J values and the spin state, 25/2 for **3** and 21/2 for **4**, obtained from the fitting process further confirm the coupling nature between the metal centers bridged by cyanide groups.

Similar to the situation in **1** and **2**, the field-dependent magnetization of **3** and **4** also presents the sigmoid shape expected for metamagnets, Figure S13 (Supporting Information), which have also been found recently in other cyanide-bridged [Mn^{III}Schiff-base]−M^{III} (M = Fe and Cr) compounds.[42,43] To confirm the magnetic phase transition for these two complexes, both FCM measurement and ac magnetic susceptibility measurement (under the same experimental conditions as for **1** and **2**) were performed, and the results are shown in the insets of Figure 10 and Figures S14 and 15 (Supporting Information). An abrupt increase under a magnetic field of 30 KOe (critical field) in the magnetization is observed at ca. 7.5 K for **3** and ca. 7.0 K for **4**. In addition, the peak at about 7.5 K for **3** and 7.2 K for **4** can also be found from the ac curves, indicating the phase transition at this temperature. Furthermore, the metamagnetic behavior for both **3** and **4** can also be testified to by their hysteresis loops, Figure 11 and Figure S12 (Supporting Information).

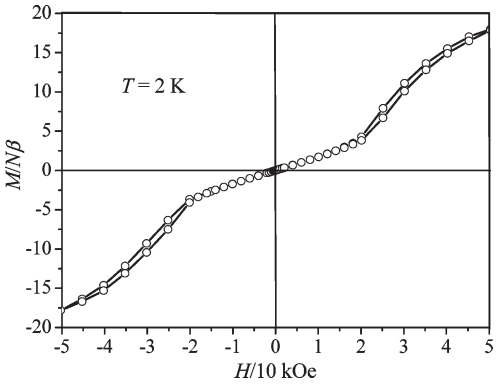

Figure 11. Magnetic hysteresis loop for complex **3** at 2 K.

Investigation over the magnetic properties of **1**−**4** reveals some characteristics of metamagnets for all four polynuclear clusters. Since the metamagnetic behavior has not been revealed for other cyanide-bridged polynuclear Fe^{III}−Mn^{III} and Cr^{III}−Mn^{III} complexes possessing similar skeleton structures to that for **1**−**4** but containing no intermolecular hydrogen-bond interactions,[22e,36] the metamagnetic behavior for **1**−**4** is attributed to the relatively strong magnetic exchange coupling through the intermolecular hydrogen-bond interaction. It is worth noting that a similar phenomenon that the magnetic property of the complexes can be mediated by the exchange coupling of transition metal ions through

(39) Feng, Y. H.; Wang, C.; Xu, G. F.; Ouyang, Y.; Liao, D. Z.; Yan, S. P. *Inorg. Chem. Commun.* **2008**, *11*, 341.
(40) Choi, H. J.; Sokol, J. R.; Long, J. R. *J. Phys. Chem.* **2004**, *65*, 839.
(41) Pan, F.; Wang, Z. M.; Gao, S. *Inorg. Chem.* **2007**, *46*, 10221.
(42) Visinescu, D.; Toma, L. M.; Lloret, F.; Fabelo, O.; Ruiz-Péez, C.; Julve, M. *Dalton. Trans.* **2008**, 4103.
(43) Visinescu, D.; Toma, L. M.; Lloret, F.; Fabelo, O.; Ruiz-Péez, C.; Julve, M. *Dalton. Trans.* **2009**, 37.

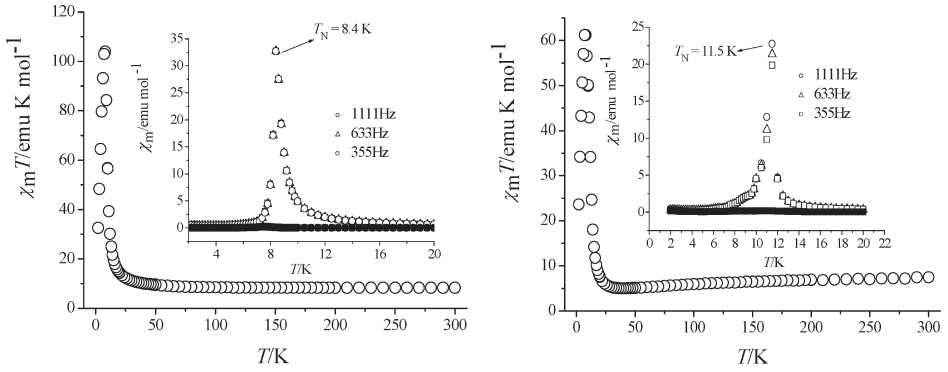

Figure 12. Temperature dependence of $\chi_m T$ for complex **5** (left) and complex **6** (right). Inset: Temperature dependence of the ac magnetization in zero static field and an ac field of 3 Oe at 355, 633, and 1111 Hz. The white and black marks represent the real and imaginary part of the ac magnetic measurement, respectively.

hydrogen bonds was revealed for other transition metal systems, in particular, the copper and nickel complexes.[44,45]

Magnetic Properties of Complexes 5 and 6. The magnetic susceptibilities of **5** and **6** were measured from 2 to 300 K under an applied magnetic field of 2000 Oe, and their temperature dependence of $\chi_m T$ is shown in Figure 12. The $\chi_m T$ value per Mn_2Fe for **5** at room temperature is 7.28 emu K mol^{-1}, obviously higher than the spin-only value of 6.38 emu K mol^{-1} for two high-spin Mn(III)'s (S = 2) and one low-spin Fe(III) (S = 1/2) on the basis of g = 2.0. For complex **6**, the corresponding value is 7.45 emu K mol^{-1}, slightly lower than the spin-only value of 7.88 emu K mol^{-1} for two uncoupled high-spin Mn(III)'s (S = 2) and one Cr(III) (S = 3/2) on the basis of g = 2.00. When the temperature is lowered, the $\chi_m T$ value for these two complexes changes smoothly from 300 to 25 K and then sharply increases to a maximum as high as 103.96 emu K mol^{-1} at 8 K for **5** and 61.19 emu K mol^{-1} at 7 K for **6**, strongly suggesting the occurrence of a three-dimensional magnetic ordering. After this, the $\chi_m T$ value decreases to a minimum value of 32.56 emu K mol^{-1} for **5** and 23.62 emu K mol^{-1} for **6** at 2 K due to the gradual saturation, suggesting the presence of interlayer antiferromagnetic coupling. The maximum $\chi_m T$ value of **5** (103.96 emu K mol^{-1}) is significantly larger than that derived from the largest possible spin state, S_T = 9/2 ($S_{Mn}(2)$, $S_{Fe}(1/2)$, $S_{Mn}(2)$), while the minimum $\chi_m T$ value of **6** is close to a spin-only value of 4.38 emu K mol^{-1} for S_T = 5/2 expected for the system of $S_{Mn}(2)$, $S_{Cr}(3/2)$, and $S_{Mn}(2)$. These data, in combination with the Weiss constant obtained below, suggest the overall ferromagnetic coupling in **5** and antiferromagnetic coupling in **6**.[22b,46] The magnetic susceptibility of these two complexes conforms well to Curie−Weiss law in the range of 15−300 K and gives the positive Weiss constant θ = 6.84 K and Curie constant C = 6.60 emu K mol^{-1} for **5** and θ = −7.46 K and C = 7.22 emu K mol^{-1} for **6**.

As revealed by the X-ray analysis, in the 2D layer structures of **5** and **6**, two types of exchange paths, namely, the intratrimer or intertrimer path between Mn(III) and Fe(III) ions through the bridging cyanide group for both **5** and **6** as well as the intertrimer path between the Mn(III) ions through the hydrogen bond in **5** and coordinated K^+ ion in **6**, exist between the metal centers within each layer. Magnetic coupling through the former path leads to a ferromagnetic nature for **5** but a antiferromagnetic one for **6**, as detailed above. As expected, interaction through the second path in both **5** and **6** is relatively weak in comparison with the magnetic exchange through the bridging cyanide group.

To confirm the magnetic phase transition, the FCM curves were also measured for both complexes, Figures S16 and 17 (Supporting Information). An abrupt increase in the magnetization can be found at about 8.4 K for **5** and 11.5 K for **6**, where the remanent magnetization vanishes, indicating that an antiferromagnetic phase transition exists at 8.4 K for **5** and 11.5 K for **6**, respectively. In the real part of the ac magnetic susceptibility measurement carried out in a 3.0 Oe ac field oscillating at 355−1111 Hz with a zero dc field (inset of Figure 12), a maximum was also observed at about 8.4 K for **5** and 11.5 K for **6**, respectively. However, no signal was observed in the imaginary part of the ac magnetic susceptibility measurement. These results confirm again the 3D antiferromagnetic ordering for these two complexes with the Neel temperature (T_N) at about 8.4 K for **5** and 11.5 K for **6**. The field-dependent magnetization for **5** and **6** shows a similar changing tendency, which first increases slowly with the external field because of the antiferromagnetic interlayer interaction, then increases rapidly at low magnetic fields, and then increases with a realtively slow speed until the field up to 50 kOe is reached, a typical characteristic of a metamagnet. The hysteresis loop at 2 K, inset of Figure 13, is evident with the coercive field of 520 Oe and the remnant magnetization of 3.87 Nβ for **5** and 490 Oe and 3.40 Nβ for **6**, respectively, further confirming their metamagnetic character.

Investigation over the magnetic properties of the six cyanide-bridged MMn (M = Fe, Cr) complexes reveals the ferromagnetic coupling between the Fe^{III} and Mn^{III} bridged by cyanide groups in all four cyanide-bridged $Fe^{III}Mn^{III}$ complexes and antiferromagnetic coupling between the cyanide-bridged Cr^{III} and Mn^{III} in the two

(44) Van Langenberg, K.; Batten, S. R.; Berry, K. J.; Hockless, D. C. R.; Moubaraki, B.; Murray, K. S. *Inorg. Chem.* **1997**, *36*, 5006.
(45) Manson, J. L.; Schlueter, J. A.; Funk, K. A.; Southerland, H. I.; Twamley, B.; Lancaster, T.; Blundell, S. J.; Baker, P. J.; Pratt, F. L.; Singleton, J.; McDonald, R. D.; Goddard, P. A.; Sengupta, P.; Batista, C. D.; Ding, L.; Lee, C. H.; Whangbo, M. H.; Franke, I.; Cox, S.; Baines, C.; Trial, D. *J. Am. Chem. Soc.* **2009**, *131*, 6733.
(46) Miyasaka, H.; Okava, H.; Matsumoto, N. *Mol. Cryst. Liq. Cryst.* **1999**, *335*, 303.

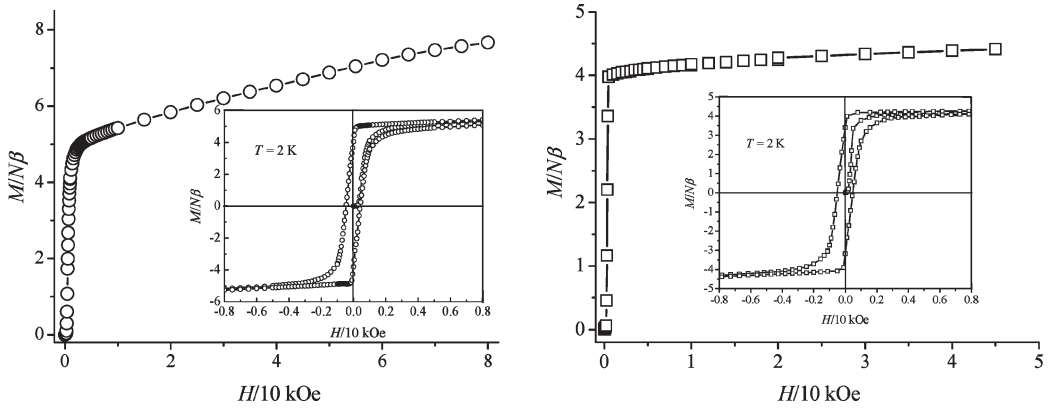

Figure 13. Field dependence of magnetization at 2 K for complexes **5** (left) and **6** (right). The insets show their hysteresis loop at 2 K.

$Cr^{III}Mn^{III}$ complexes. The present result is in agreement with the fact that most cyanide-bridged $Mn^{III}-Fe^{III}$ complexes were revealed to exhibit ferromagnetic interaction with few exceptions, and a few cyanide-bridged $Cr^{III}Mn^{III}$ complexes usually show antiferromagnetic coupling, Table S3 and S4 (Supporting Information). The present result not only provides new cyanide-bridged complexes for the purpose of elucidating the magneto-structure correlation in molecular magnetic materials but also confirms the much more usual ferromagnetic $Fe^{III}-Mn^{III}$ coupling and antiferromagnetic $Cr^{III}-Mn^{III}$ coupling through cyanide bridges.

Conclusion

In summary, a new series of heterobimetallic cyanide-bridged polynuclear clusters and 2D coordination polymers have been designed and synthesized using three polycyanidemetalates and two manganese(III) compounds containing bicompartmental Schiff base ligands as building block. The number of charges and cyanide groups of polycyanidemetlates and the position and size of the substituted group on the Schiff base ligand have been revealed to play an important role in determining the structure of resulting complexes. Investigation over their magnetic properties reveals an overall ferromagnetic coupling for complexes **1**, **2**, and **3** and antiferromagnetic coupling for **4** between the Mn(III) and Fe(III)/Cr(III) ions bridged by cyanide groups. The metamagnetic behavior revealed for **1**−**4** at low temperatures is attributed to the relatively strong intermolecular hydrogen-bond interaction. Both **5** and **6** with a two two-dimensional layer structure display the three-dimensional antiferromagnetic ordering with typical metamagnetic character.

Acknowledgment. This work was supported by the National Natural Science Foundation of China (Grant No. 20931001 and 20701027).

Supporting Information Available: Crystallographic data in CIF format. The anionic crystal structure and one-dimensional double-chain structure of complex **2**. The asymmetry cationic unit, heptanuclear cationic crystal structure, and 3D supermolecular structure of complex **4**. The trinuclear structure, 2D network structure, and cell packing diagram of complex **6**. The temperature dependence of $\chi_m T$, field-cooled magnetization, and magnetic hysteresis loop for complex **2**. The field dependence of magnetization at 2 K for complexes **1**−**4**. Magnetic hysteresis loop for complex **4**. Temperature dependence of ac magnetization of complexes **1**, **3**, and **4**. Field-cooled magnetization of complexes **5** and **6**. Selected hydrogen-bond parameters in complexes **1**−**4** and bond lengths and angles for complexes **5** and **6**. Comparison of the magnetic property of cyanide-bridged $Fe^{III}Mn^{III}$ and $Cr^{III}Mn^{III}$ complexes. This material is available free of charge via the Internet at http://pubs.acs.org.